6641

Photoinduced Electron Transfer and Subsequent Chemical Reactions of Adsorbed Thianthrene on Clay Surfaces

Yun Mao and J. Kerry Thomas*

Department of Chemistry and Biochemistry, University of Notre Dame, Notre Dame, Indiana 46556

This study reports data on the photoinduced electron transfer of thianthrene on clay, laponite, surfaces. Diffuse reflectance and fluorescence spectroscopy studies show that adsorbed thianthrene molecules interact with the clay surface in two ways, a physical interaction which leads to a spectral perturbation and a chemical interaction which leads to ground-state surface complexes with charge-transfer (CT) character. Time-resolved fluorescence studies indicate that thianthrene is adsorbed at various surface sites resulting in nonexponential fluorescence decay. Photoirradiation of the CT surface complexes induces electron transfer leading to radical cations, $Th^{\bullet+}$, which are observed by diffuse reflectance and EPR spectroscopy. Recombination of the electron-ion pairs is observed on warming samples initially irradiated at low temperatures. A subsequent photoirradiation leads to further reaction of $Th^{\bullet+}$. Product analysis confirms that on irradiation into its surface CT band thianthrene is photochemically oxidized, that the mechanism is free radical in nature, and that the important reaction of $Th^{\bullet+}$ on clay surfaces is hydrolysis.

Introduction

The photochemical properties of organic molecules are markedly influenced when the molecules are adsorbed on solid surfaces. Luminescence, diffuse reflectance, and EPR spectroscopy, either steady-state or time-resolved, provide valuable information about the nature of organic-surface interactions.[1-15] These studies monitor the surface properties, e.g., the polarity and the electron affinity of the surface sites; they also characterize the behavior of the organic adsorbates, e.g., molecular conformation, formation of surface complexes, and photoinduced electron transfer.

Clay and clay minerals are widespread materials in the environment, and many organic pollutants are often deposited or adsorbed on clay surfaces. From this respect, chemical reactions on restricted surfaces are of immediate interest.[11,16,17] Early thermal studies showed the formation of radical cations and anions of aromatic compounds on active alumina and silica–alumina.[1,2] Recently, a growing

interest has developed in photoinduced processes of organic adsorbates on clay surfaces, perturbation of adsorbate adsorption and emission spectra, charge-transfer complexes, photoinduced electron transfer, and subsequent reactions of radical species. However, a complete understanding of the photochemical reactions on clay surfaces is not established. For example, the fate of photogenerated electrons is not well clarified, although in some cases trapped electrons were observed.[18]

In this paper thianthrene (Th) was selected as a model compound; its structure is shown in Scheme I, and it was adsorbed on sodium laponite (hereafter referred to as laponite), a synthetic clay with a similar structure to that of hectorite. Electron-transfer studies of thianthrene in homogeneous systems and subsequent reactions of ions have been reported.[19,20] This report gives details of spectroscopic observations and product analysis which provide insight into the photochemical reactions of thianthrene on the clay surface.

Experimental Section

Chemicals. Thianthrene from Aldrich (99%) was used as received without further treatment, and its purity was monitored using HPLC analysis. Sodium laponite (RDS) was received from Laporte Industries. The composition of the laponite, as supplied by the producer, is as follows: SiO_2, 55.6%; MgO, 25.1%; Na_2O, 3.6%; Li_2O, 0.7%; K_2O, 0.2%; TiO_2, 0.15%; Al_2O_3, 0.08%; CaO, 0.06% and Fe_2O_3, 0.04%. Most of the studies were done with laponite preheated at 130 °C (T_a = 130 °C, T_a is the activation temperature), unless otherwise noted. Thianthrene radical cation perchlorate ($Th^{\bullet+}ClO_4^-$) was prepared as described in the literature.[21,22] Thianthrene 5-oxide (ThO) was prepared by using hydrolysis of $Th^{\bullet+}ClO_4^-$ in acetonitrile. The remaining chemicals were of highest purity available.

Instrumentation. A UV–visible spectrophotometer (Perkin-Elmer 552) equipped with an integrating sphere accessory was used to measure diffuse reflectance spectra. The spectra were recorded as $-\log R_T$ versus wavelength, where R_T is the relative diffuse reflectance of thick samples; R_T and $-\log R_T$ are used at

[●] Abstract published in *Advance ACS Abstracts*, November 1, 1993.

(1) Rooney, J. J.; Pink, R. C. *Trans. Faraday* 1962, 1632.

(2) Flockhart, B. D.; Leith, I. R.; Pink, R. C. *J. Catal.* 1967, *9*, 45.

(3) de Mayo, P.; Natarajan, L. V.; Ware, W. R. In *Organic Photo-transformations in Nonhomogeneous Media*, ACS Symp. Ser. 278; Fox, M. A., Ed.; American Chemical Society: Washington, DC, 1984; p 1.

(4) Oelkrug, D.; Krabichler, G.; Honnen, W.; Wilkinson, F.; Willsher, C. J. *J. Phys. Chem.* 1988, *92*, 3589.

(5) Oelkrug, D.; Flemming, W.; Fuellerman, R.; Guenther, R.; Honner, W.; Krabichler, G.; Schafer, M.; Uhl, S. *Pure Appl. Chem.* 1986, *58*, 1207.

(6) Oelkrug, D.; Erbse, H.; Plauschinat, M. *Z. Phys. Chem. (N.F.)* 1975, *96*, 283.

(7) Oelkrug, D.; Plauschinat, M.; Kessler, R. W. *J. Luminescence* 1975, *18/19*, 434.

(8) Oelkrug, D.; Radjaipour, M. *Z. Phys. Chem. (N.F.)* 1980, *123*, 163.

(9) Honnen, W.; Krabichler, G.; Uhl, S.; Oelkrug, D. *J. Phys. Chem.* 1983, *87*, 4872.

(10) Oelkrug, D.; Krabichler, G.; Honnen, W.; Wilkinson, F.; Willsher, C. J. *J. Phys. Chem.* 1988, *92*, 3589.

(11) (a) Thomas, J. K. *Acc. Chem. Res.* 1988, *21*, 275. (b) Thomas, J. K. *Chem. Rev.* 1993, *93*, 301 and references therein.

(12) Pankasem, S.; Thomas, J. K. *J. Phys. Chem.* 1991, *95*, 6990.

(13) Pankasem, S.; Thomas, J. K. *J. Phys. Chem.* 1991, *95*, 7385.

(14) Liu, X.; Thomas, J. K. *Langmuir* 1991, *7*, 2808.

(15) Liu, X.; Iu, K.-K.; Thomas, J. K. *Langmuir* 1992, *8*, 539.

(16) Theng, B. K. G. *The Chemistry of Clay-Organic Reactions*; John Wiley & Sons: New York, 1974.

(17) Ballantine, J. A. In *Chemical Reactions in Organic and Inorganic Constrained Systems*, NATO ASI C ser. vol. 165; Setton, R., D., Ed.; Reidel Publishing Co.: 1985; p 197.
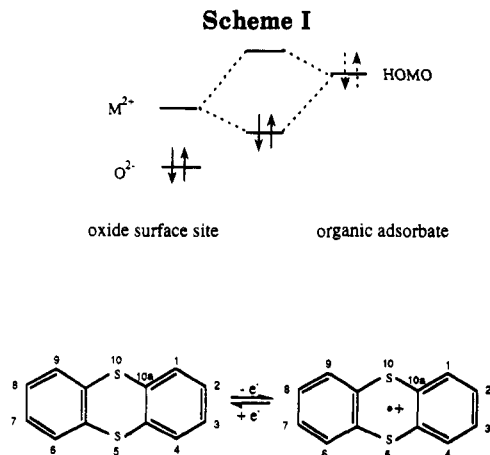
(18) Iu, K. K.; Thomas, J. K. *J. Phys. Chem.* 1991, *95*, 506.

(19) Shin, S. R.; Shine, H. J. *J. Org. Chem.* 1992, *57*, 2706.

(20) Jones, G., II; Huang, B.; Griffin, S. F. *J. Org. Chem.* 1993, *58*, 2035.

(21) Lucken, E. A. *J. Chem. Soc.* 1962, 4963.

(22) Murada, Y.; Shine, H. J. *J. Org. Chem.* 1969, *34*, 3368.

Scheme I

oxide surface site   organic adsorbate

low absorbance instead of the Kubelka–Munk function $f(R)$ to express absorption spectra.[23,24] In order to estimate the yield of ionic thianthrene species, the synthesized $Th^{•+}ClO_4^-$ salt was loaded on dry laponite powder and the diffuse reflectance R_T was measured. According to the relationship

$$f(R_T) = (1 - R_T)^2/2R_T = 2\gamma_0 C, \qquad (1)$$

where C is the loading concentration of $Th^{•+}ClO_4^-$, the proportional constant γ_0 was determined under the known loading concentrations and is used later to assess the yield.[25]

Steady-state emission was measured on a spectrofluorometer (Perkin-Elmer, MPF 44-B). The phosphorescence lifetimes were measured using phosphoroscopy. The thermal chemiluminescence was recorded on a spectrofluorometer (SLM Aminco, SPF 500) in a fast scanning mode (10 nm/s). EPR spectra were recorded on an electron paramagnetic resonance spectrometer (Varian Associate, E-lines century series) equipped with an X-band klystron and a TE_{102} type cavity, and the g value was determined by comparison with DPPH (2,2-diphenyl-1-picrylhydrazine). Samples for EPR measurements were contained in 5-mm o.d. quartz tubes connected to wider glass tubing that was attached directly to a vacuum line.

Samples for time-resolved emission studies were excited with an Nd-YAG synchronously pumped, mode-locked, and cavity dumped dye laser (Continuum, PY61-10), using the fourth harmonic 266 nm (0.1 mJ/pulse, 20 ps FWHM). The emission from these samples was transferred to a monochromator via a lens system and detected by a microchannel plate tube. The output of the microchannel plate tube was coupled to a programmable digitizer (Tektronix 7912AD) with an amplifier plug in (Tektronix 7A29). In order to remove the interference of the laponite solid matrix, the detection system was optimized so that the background of the laponite solid matrix was negligible. Time-resolved diffuse reflectance and transmission spectra were measured by laser flash photolysis. A 308-nm laser pulse (70 mJ/cm², 10 ns FWHM) from a XeCl excimer laser (Lambda Physik, Model EMG 100) was used for solid samples, a 337-nm laser pulse (150 mW/cm², 10 ns FWHM) from a N_2 laser (Laser Photonics, UV24) was used for liquid samples, and a 450-W xenon lamp was used as the analyzing light source. The monitoring light from the samples was transferred to a monochromator by an optical fiber or a lens system and detected by a photomultiplier tube. The output of the photomultiplier was coupled to a programmable digitizer (Tektronix 7912AD) with differential comparator plug in (Tektronix 7A13), connected to a Zenith data system.

Steady-state photoirradiation was carried out either in a photoreactor equipped with a merry-go-round and RPR 3000 Å/3500 Å lamps (Rayonet, Southern New England Co.) or with a 150-W xenon lamp. The photoirradiation intensities were measured with the chemical actinometer $K_3Fe(C_2O_4)_3$.

(23) Hecht, H. G. In *Modern Aspects of Reflectance Spectroscopy*; Interscience Publisher: New York, 1968; p 1.
(24) Kortüm, G. *Reflectance Spectroscopy*; Spring-Verlag: New York, 1969.
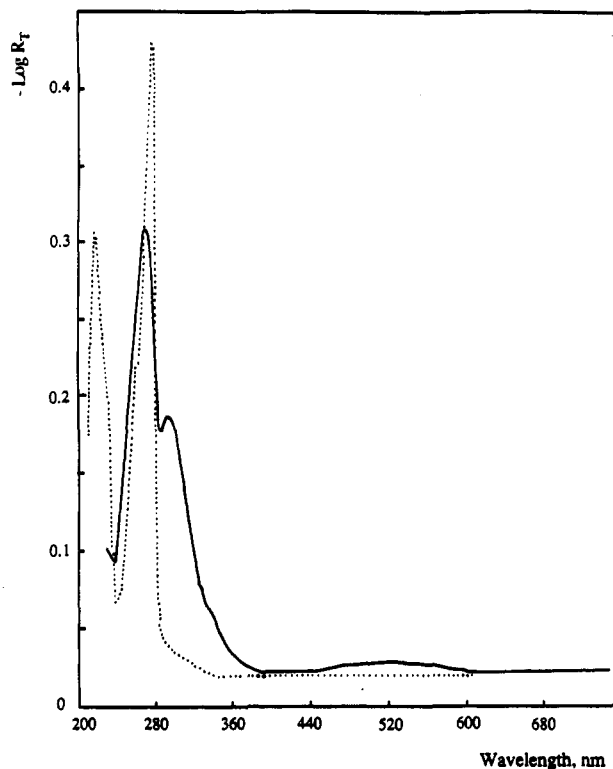(25) Hecht, H. G. *Anal. Chem.* **1976**, *48*, 1775.

Wavelength, nm

Figure 1. Diffuse reflectance spectrum of thianthrene on a laponite surface (solid line), measured at room temperature; thianthrene loading concentration was 2.0×10^{-6} mol/g. For comparison, an absorption spectrum of thianthrene in cyclohexane is included (dotted line).

Sample Preparations. Laponite powder (1.0 g) in quartz crucibles was heated for 20 h under air at selected temperatures, 130 or 325 °C. After thermal activation, the powdered samples were cooled in a desiccator to room temperature and mixed with 0.5–2.0 mL of 10^{-3} M thianthrene in dry cyclohexane. Under these conditions 99% of thianthrene is adsorbed on the laponite surface. The samples were used for diffuse reflectance and EPR spectroscopy after drying in a stream of N_2.

After photoirradiation, the samples were extracted with aerated aqueous acetonitrile. Samples for HPLC were first centrifuged to remove any powder and then filtered through a Millipore frit (0.45 μm). Separation and identification of chemical products were performed by a Waters' high performance liquid chromatograph which was equipped with a Nova Pak C_{18} column and UV-absorption detector; the eluent consisted of aqueous acetonitrile solution.

Results and Discussion

1. Characteristics of the Adsorbed Thianthrene Molecule. Figure 1 shows a diffuse reflectance spectrum of thianthrene adsorbed on a laponite surface. Strong bands at 265 and 290 nm are observed, together with a weak broad band in the region of 450–600 nm. A comparison of the absorption bands of thianthrene on the surface to those in solution (dotted line in Figure 1) shows that the band at 265 nm results from the adsorbed thianthrene molecules, and a slight structure which appears in solution is obscured. The weak broad band in the range of 450–600 nm is ascribed to a trace amount of radical ions, which shows a thermal reaction on laponite surfaces and will be discussed later.

The band at 290 nm with a tail into the region of 300–400 nm is assigned to charge-transfer (CT) complexes, where the thianthrene molecules act as electron donors
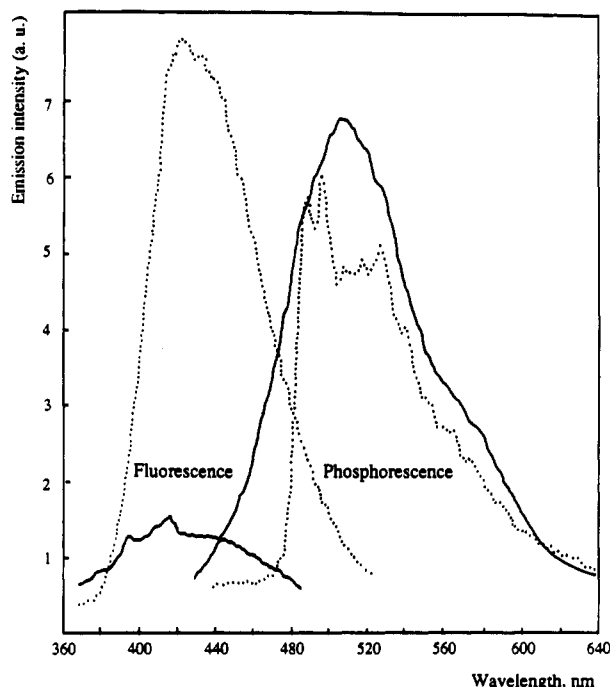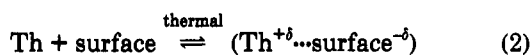
Figure 2. Steady-state luminescence spectra of thianthrene samples. Solid line: thianthrene/laponite samples, 2.0 × 10⁻⁶ mol/g. Dotted line: thianthrene in isopentane, 1.0 × 10⁻⁴ M. The fluorescence spectra were recorded at room temperature, with an excitation wavelength of 250 ± 10 nm. The phosphorescence spectrum of thianthrene/laponite sample was recorded at room temperature and at −196 °C for thianthrene in isopentane; the excitation source was a 150-W xenon lamp with a UV bandpass filter (260–380 nm).

Table I. Average Lifetimes of Phosphorescence[a] of Thianthrene Molecules in Isopentane Glass and on Solid Surfaces

	at 20 °C, τ, ms	at −196 °C, τ, ms
Th/isopentane[b]	–	26.0 ± 2.0
Th/laponite[c]	7.5 ± 0.75	33.2 ± 3.0

[a] The lifetimes of phosphorescence were measured in the first 20 ms; all samples were degassed. [b] The concentration of thianthrene in isopentane was 2.0 × 10⁻⁴ M. [c] The loading concentration was 1.0 × 10⁻⁶ mol/g.

steady-state emission spectra of thianthrene/laponite samples. The fluorescence of thianthrene adsorbed on surfaces is weak and is just distinguishable above the background; an average lifetime of the fluorescence on solid is measured as 7.9 ns. Under the same conditions thianthrene in solution shows an unstructured band at 432 nm (dotted line in Figure 2) with an average lifetime of 29 ns. The low yield and short lifetime of the fluorescence is indicative that there is a fast relaxation process of the excited states on the solid surface.

The phosphorescence of thianthrene/laponite samples, measured at room temperature, shows an unstructured emission band at 510 nm. By comparison with the spectrum in isopentane glass measured at −196 °C (cf. right portion of Figure 2), the band at 510 nm is identified as the phosphorescence of adsorbed thianthrene molecules. The average lifetime of the phosphorescence is measured using phosphoroscopy and summarized in Table I. The lifetimes of thianthrene/isopentane and thianthrene/laponite samples at −196 °C are comparable. However, at room temperature the fluid samples do not show observable phosphorescence, while the phosphorescence of solid samples is observable with a lifetime of 7.5 ms.

Figure 3 exhibits time-resolved emission data taken at 420 nm. The time-domain data exhibit two characteristics: the decay of excited states on the surface is faster than that in solution and deviates from monoexponential kinetics, while the decay of excited thianthrene in cyclohexane solution is monoexponential with a rate constant of 3.5 × 10⁷ s⁻¹. The faster decay of the emission on the surface indicates an interaction between the excited states and the microenvironment. As shown in Figure 3, the time profile of the 420-nm band on the surface is fitted well by a Gaussian distribution model,[29-31]

and electron-deficient surface sites act as electron acceptors.

$$\text{Th} + \text{surface} \overset{\text{thermal}}{\rightleftharpoons} (\text{Th}^{+\delta}\cdots\text{surface}^{-\delta}) \qquad (2)$$

The concept of the CT complexes is well established, and the formation of adsorbate–surface complexes in several heterogeneous systems has been reported.[6-10,26,27] The CT complexes are characterized by new broad absorption bands near the red edge of the parent compounds. Supporting evidence for this assignment is that steady-state photoirradiation into the CT band generates ionic species (*vide infra*).

The formation of the CT surface complex and its characteristic UV–visible spectrum may be understood on the basis of the localized-bond molecular orbital model,[28] which is schematically shown in Scheme I. The populated orbital (often the highest occupied molecular orbital, HOMO) of the absorbates interacts with the electron-deficient atomic orbital of the surface metal cation (M²⁺), resulting in a localized electron-pair bond accompanied by the appearance of new antibonding intermolecular orbitals of the complexes. The latter exhibits an absorption band at the red edge of the parent compounds.

Emission spectroscopy provides further information about the interaction of the adsorbed thianthrene molecules with their microenvironment. Figure 2 shows the

$$\frac{I_t}{I_0} = \pi^{-1/2} \int_{-\infty}^{+\infty} \exp(-x^2)\, \exp[-\bar{k}t\, \exp(\gamma x)]\, dx \qquad (3)$$

with $x = (\ln k - \ln \bar{k})/\gamma$; x denotes the dispersion of the rate constant, its range is $-\infty < x < +\infty$, γ is the width of the distribution, k and $\bar{k}$ are the rate constant and its average, and I_t and I_0 are the fluorescence intensities at time t and $t = 0$, respectively. If Th molecules adsorb on specific sites of one type, γ will be zero. The Gaussian fitting of the decay gives an average rate constant of 1.27 × 10⁸ s⁻¹ and a width of 0.884. This shows that the organic adsorbate molecules adsorb on different surface sites. This result is consistent with earlier work.[12,30,31]

2. Photoinduced Electron Transfer of Thianthrene on Laponite Surfaces. Photoirradiation of thianthrene/

(26) Mao, Y.; Thomas, J. K. *J. Chem. Soc. Faraday Trans.* **1992**, *88*(20), 3079.

(27) (a) Mao, Y.; Thomas, J. K. *Langmuir* **1992**, *8*, 2501. (b) Mao, Y.; Pankasem, S.; Thomas, J. K. *Langmuir* **1993**, *9*, 1504.

(28) Cunningham, J. In *Surface and Near-Surface Chemistry of Oxide Materials*; Nowotny, J., Dufour, L. C., Eds.; Elsevier Science B. V.: Amsterdam, 1990; p 345.

(29) Albery, W. J.; Bartlett, P. N.; Wilde, C. P.; Darwent, J. R. *J. Am. Chem. Soc.* **1985**, *107*, 1854.

(30) Hite, P.; Krasnansky, R.; Thomas, J. K. *J. Phys. Chem.* **1986**, *90*, 5765.

(31) Krasnansky, R.; Koike, K.; Thomas, J. K. *J. Phys. Chem.* **1990**, *94*, 4521.
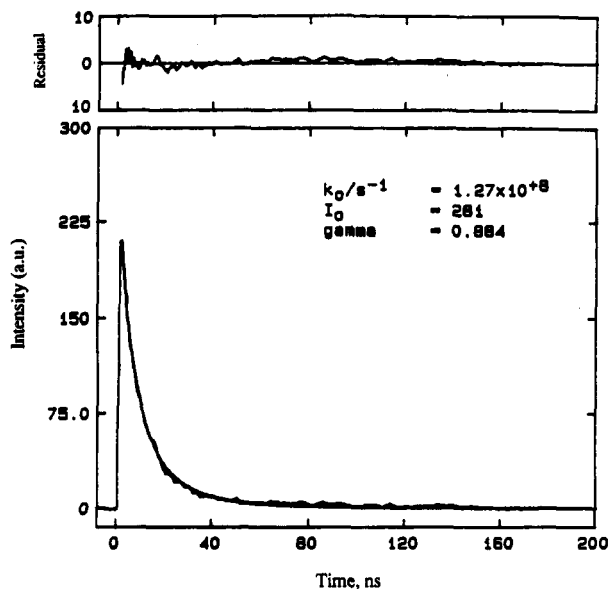
Figure 3. Time-resolved fluorescence decay of the solid sample measured at room temperature (monitored at 420 nm), degassed solid sample with a thianthrene loading of 2.0×10^{-6} mol/g. Jagged line: experimental data. Smooth line: Gaussian distribution fitting (see text). At the top in the figure, the residual of the fitting is presented.

Figure 4. Diffuse reflectance spectrum of thianthrene/laponite measured at room temperature. Samples were irradiated with RPR 3500-Å lamps at room temperature. Irradiation time, from bottom to top: 0, 2.0, 5.0, 10.0 and 20.0 min. A thianthrene loading of 2.0×10^{-6} mol/g was used.

laponite samples with UV light (RPR 3500 Å) at room temperature initiates photochemical reaction of thianthrene, giving rise to a color change of the sample from white to pink. As shown in Figure 4, the diffuse reflectance spectrum exhibits a strong band centered at 545 nm and a band at 300 nm with some structure which is superimposed on that of the parent compound. The intensities of both bands gradually increase with time of irradiation. The bands at 300 and 545 nm are identical to the absorption spectrum of $Th^{\bullet+}ClO_4^-$ in dry acetonitrile and are ascribed to thianthrene radical cations ($Th^{\bullet+}$). This assignment is also consistent with early reports of $Th^{\bullet+}$ in solution.[32,33]

$$(Th^{+\delta}\text{···surface}^{-\delta}) \xrightarrow{\text{CT-}h\nu/\text{RT}} (Th^{\bullet+}/\text{surface}^-) \qquad (4)$$
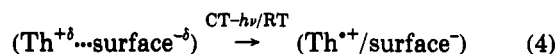
Steady-state irradiation with a wavelength ($\sim$350 nm) that is at lower energy than that of the absorption band of thianthrene initiates electron transfer. The photoinduced ionization occurs in both aerated and degassed samples. This datum is evidence for ground-state surface CT complexes, which on excitation give ions. With multichromatic irradiation with wavelengths of 280–350 nm and at an intensity of 4×10^{-3} einstein/min cm^2, ca. 3–4% of thianthrene in a sample, loading of 1×10^{-6} mol/g, is converted into $Th^{\bullet+}$ during the first minute. Under monochromatic irradiation with a wavelength of 320 ± 2 nm and an intensity of 1.8×10^{-6} einstein/min, a quantum yield for the generation of $Th^{\bullet+}$ was calculated according to eq 1, $\Phi_{Th^{\bullet+}} = 0.035\%$. The low quantum yield is typical of excitation of CT complexes and has been observed in other photoinduced charge-transfer systems.[34] It has been concluded that dissociation into free ions from an initial geminate pair does not compete favorably with charge recombination. Evidence for recombination of ion-elec-
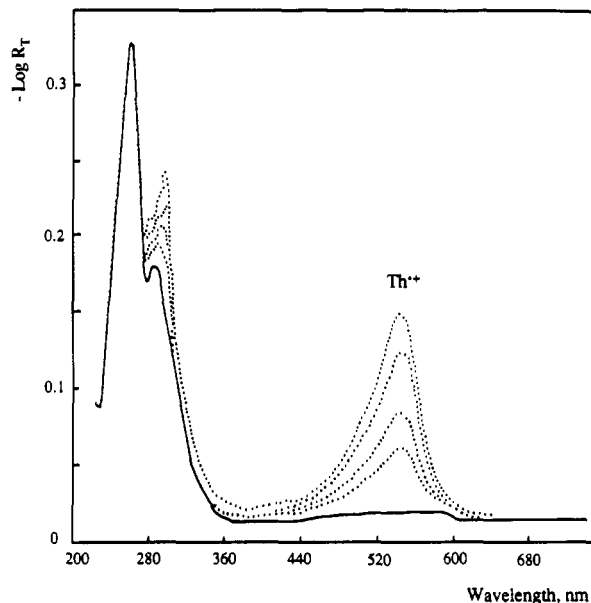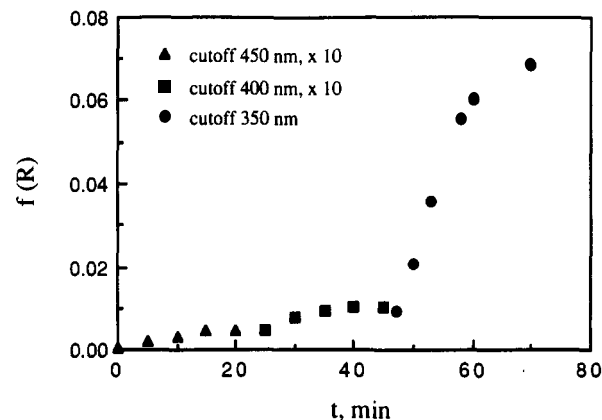

Figure 5. Effect of photoenergy on the $Th^{\bullet+}$ yield. $f(R)$ was used as the relative yield measured by diffuse reflectance spectroscopy. Photon source was a 150-W Xe lamp. The photoenergies were adjusted by cutoff filters as shown in the legends. For cutoff filter/450, 400, and 350 nm, the zero transmission points are 431, 367, and 330 nm, respectively.

tron pairs will be given later in the section on the observation of thermal chemiluminescence. The light scattering of the solid samples also tends to decrease the quantum yield.

The energy and intensity of the photoirradiation are important parameters for photoinduced electron transfer and provide information on the nature of the electron-transfer process. Figure 5 exhibits the effect of the photoenergy on the $Th^{\bullet+}$ yield. The photoenergy was adjusted with cutoff filters. Irradiation with wavelengths $\lambda > 450$ nm generates a low $Th^{\bullet+}$ yield, which rapidly approaches saturation at 25 min. Replacement of the cutoff filter to pass $\lambda > 400$ nm produces more $Th^{\bullet+}$ which also slowly reaches saturation at 45 min. Photoirradiation with higher photoenergy ($\lambda > 350$ nm) leads to a continuous increase of $Th^{\bullet+}$. These studies suggest that thianthrene molecules are not adsorbed uniformly on the clay surface. Thianthrene molecules which exist as surface complexes

(32) Fava, A.; Sogo, P. B.; Calvin, M. *J. Am. Chem. Soc.* **1957,** *79,* 1078.
(33) Shida, T. *Electronic Absorption Spectra of Radical Ions,* Physical Science Data 34; Elsevier: Amsterdam, 1988.
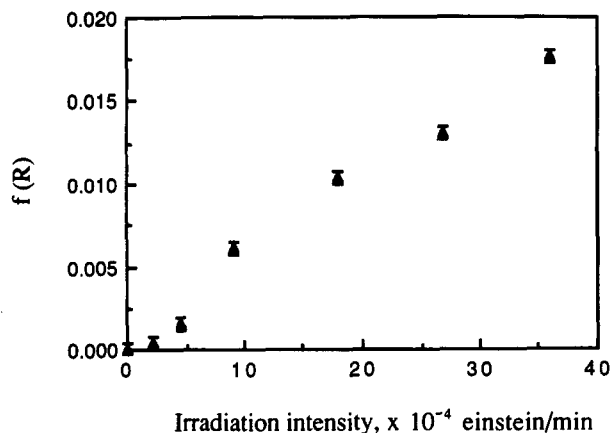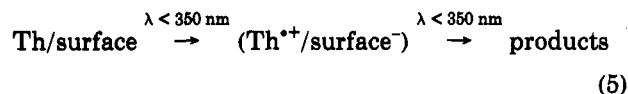(34) Mataga, N.; Shioyama, H.; Kanda, Y. *J. Phys. Chem.* **1987,** *91,* 314.

Figure 6. Dependence of Th$^{\bullet+}$ yield on the photoirradiation intensities. The samples were irradiated with RPR 3000-Å lamps for 5 min at room temperature; the relative yields were measured by diffuse reflectance spectroscopy; and the photoirradiation intensities were estimated using actinometer $K_3Fe(C_2O_4)_3$.

Figure 7. Effect of extended irradiation. Diffuse reflectance spectra were measured at room temperature; the sample was degassed and irradiated at room temperature; and irradiation time, observed at 540 nm from top to bottom, was 30, 60, 90, and 120 min.

can be ionized under lower photoenergy, while thianthrene molecules which are physically adsorbed on the surface need higher photoenergy to produce ionization. The ratio of the Th$^{\bullet+}$ yield generated with different cutoff filters is a measure of the relative amounts of the different adsorption sites. A comparison of the Th$^{\bullet+}$ yields with different filters shows that only ca. 2.0% of the thianthrene exists in a charge-transfer state.

Figure 6 shows that increasing the photoirradiation intensity leads to an approximate linear increase in the Th$^{\bullet+}$ yield. This is similar to studies of biphenyl on silica–alumina surfaces and suggests that, up to an irradiation intensity of 4×10^{-3} einstein/min cm^2, the photoionization is monophotonic in nature.[26] The monophotonic process is also confirmed by the observation that aerated samples also show comparable yields of Th$^{\bullet+}$. It is well established that O$_2$ removes long-lived intermediates, i.e., triplet states of thianthrene which might participate in the second step of a biphotonic process.

Photoirradiation of thianthrene/laponite generates the Th$^{\bullet+}$ species, while extended irradiation times ($\lambda < 350$ nm), ca. 1–2 h, lead to bleaching of the pink color of the sample. As shown in Figure 7, the band at 545 nm decreases during long term irradiation, while a new broad band in the range of 350–500 nm appears, indicating that Th$^{\bullet+}$ is converted into a species with an absorption band at 350–500 nm. Photoirradiation with wavelength $\lambda > 450$ nm does not induce bleaching.

$$\text{Th/surface} \xrightarrow{\lambda < 350\ nm} (\text{Th}^{\bullet+}/\text{surface}^-) \xrightarrow{\lambda < 350\ nm} \text{products}$$

$$(5)$$

3. Observation of the Back Electron Transfer of the Photoinduced Ion Pair.

The photoinduced electron transfer is confirmed by observation of Th$^{\bullet+}$; however, the accompanying electrons are not observed in the UV–visible spectrum. It is also difficult to distinguish the existence of electrons in EPR spectra (*vide infra*). Recombination of the ion-electron pairs provides indirect proof of the existence of reactive negative species. At low temperature, −196 °C, photoinduced Th$^{\bullet+}$ exhibits the same diffuse reflectance spectra as that at room temperature. On warming the sample, a thermal chemiluminescence with a strong band at ~510 nm and a shoulder (ca. 580 nm), together with a weak band at ~430 nm, are
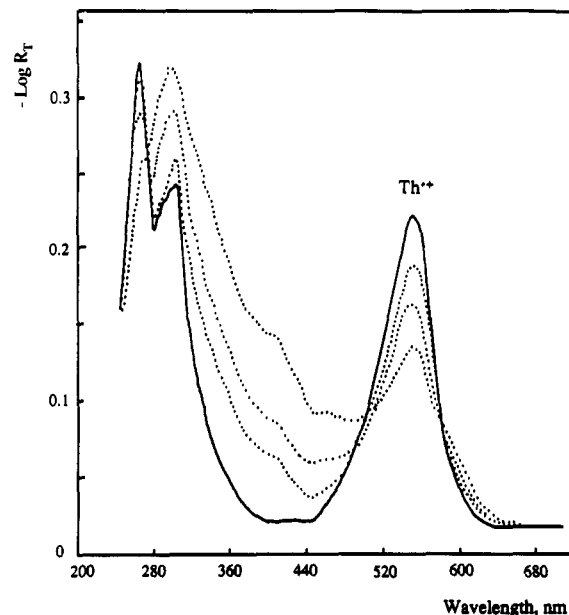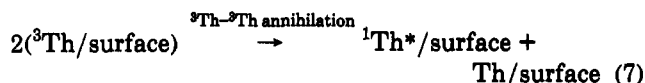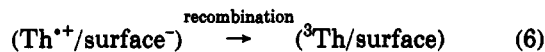
observed as shown in Figure 8a; the absorption intensity at 540 nm decreases with time of annealing (Figure 8b).

A comparison of the band position and shape with that in steady-state emission studies (*cf.* Figure 2), indicates that the thermal luminescence band at ~510 nm is the phosphorescence of thianthrene and the weak band at ~430 nm is the fluorescence of thianthrene. This thermal chemiluminescence originates from back electron transfer to Th$^{\bullet+}$. It indicates that at low temperature the photoinduced electrons are temporarily trapped on the surface in the vicinity of Th$^{\bullet+}$ and that thermal activation at room temperature leads to recombination. It is proposed that electrons also recombine rapidly with Th$^{\bullet+}$, and this initial process which is not observed in these measurements leads to a low quantum yield.

The intensity of the thermal phosphorescence is much stronger than that of the thermal fluorescent. This is a consequence of the nature of the recombination of Th$^{\bullet+}$ with electrons, which favors generation of triplet states (^{3}Th), and subsequently triplet–triplet annihilation generates excited singlet states (^{1}Th*).

$$(\text{Th}^{\bullet+}/\text{surface}^-) \xrightarrow{\text{recombination}} (^3\text{Th}/\text{surface}) \qquad (6)$$

$$2(^3\text{Th}/\text{surface}) \xrightarrow{^3Th-^3Th\ annihilation} {}^1\text{Th}*/\text{surface} + \text{Th/surface} \qquad (7)$$

The intensity of the thermal fluorescence depends on competition between phosphorescence emission and triplet–triplet annihilation of ^{3}Th. The rate of encounters of ^{3}Th species with each other is hindered by the surface adsorption. This explains the low yield of ^{1}Th*. This assignment is supported by early reports of neutralization of Wurster's blue cations[35] and other aromatic radical cations on solid surfaces.[26,27b]

(35) (a) Weller, A.; Zachariasse, K. *J. Chem. Phys.* **1967**, *46*, 4984. (b) Weller, A.; Zachariasse, K. *J. Chem. Phys. Lett.* **1971**, *10*, 197.
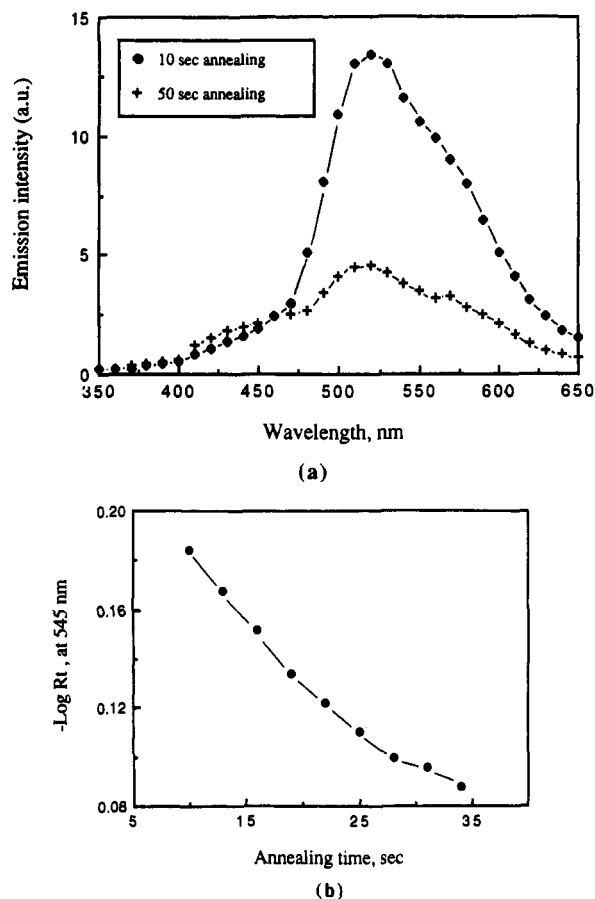
Figure 8. (a) Thermal chemiluminescence. The sample thianthrene/laponite was irradiated (RPR 3000-Å lamps) with a light intensity of $\sim 4 \times 10^{-3}$ einstein/min cm^2 for 10 min at -196 °C; the chemiluminescence was recorded with a fast scanning mode during the annealing process at room temperature. (b) Absorption intensity at 545 nm decreases with the annealing time (see text).
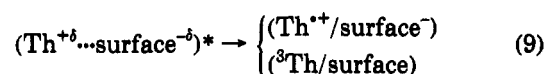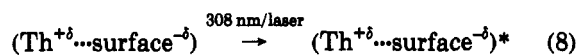
4. Observation of Laser-Induced Transient Species of Thianthrene on the Surface.

Samples were excited by a 308-nm XeCl excimer laser in the time-resolved studies, and the transient species were observed by diffuse reflectance spectrscopy. Figure 9a shows a typical time-resolved diffuse reflectance spectrum of a degassed thianthrene/laponite samples taken 50 μs, 0.50 ms, and 3.0 ms after the laser pulse. Absorption bands at 480 and 540 nm are observed.

As in steady-state studies, the band at 540 nm is ascribed to Th$^{\cdot +}$. The formation of Th$^{\cdot +}$ is a rapid process and cannot be resolved in the present detection system, limited to times ≥ 100 ns. Th$^{\cdot +}$ is stable over a time scale of several hours. The small decrease of the band at 540 nm is attributed to overlap with the band at 480 nm, which shows significant decay.

The formation of the band at 480 nm is rapid, and the band subsequently shows a decay with an average lifetime of 8.6 ± 1 ms. Only a trace at 480 nm was observed in aerated samples. These data suggest that the 480-nm band may be ascribed to triplet–triplet absorption of thianthrene. Because the average lifetime of the 480-nm band is the same as that of the phosphorescent state within the experimental error (cf. Table I), the states can be quenched by the presence of O$_2$. The assignment of the 480-nm band is further supported by an experiment of triplet–triplet transfer from benzophenone to thianthrene mol-

ecules. It is well established that triplet states of benzophenone react with other molecule via triplet–triplet transfer.[36a] Figure 9b shows the time-resolved transmission spectra taken 1.0 μs after the laser flash. The Th/benzene sample does not show any observable absorption, while the benzophenone/benzene sample shows an absorption band at 540 nm which is identified as the triplet state of benzophenone, consistent with the literature.[36b] In a mixture of thianthrene and benzophenone a new absorption band at 480 nm appears, which is ascribed to the triplet state of thianthrene (^{3}Th) generated via triplet–triplet transfer. The inset in Figure 9b shows that the band at 480 nm grows after the laser flash and is indicative of the triplet–triplet transfer process.

Accordingly, the laser-induced photolysis is summarily described as follows: the 308-nm laser pulse generates the excited CT complexes, which either ionize to form ion–electron pairs or generate locally excited states ^{3}Th/surface. The formation of ^{3}Th is a competitive process with the ionization, which can also explain why the $\Phi_{Th^{\cdot +}}$ is so low. The formation of such localized excited states in CT complexes has been observed in homogeneous systems.[37]

$$(\text{Th}^{+\delta}\cdots\text{surface}^{-\delta}) \xrightarrow{308\ \text{nm/laser}} (\text{Th}^{+\delta}\cdots\text{surface}^{-\delta})^* \quad (8)$$

$$(\text{Th}^{+\delta}\cdots\text{surface}^{-\delta})^* \rightarrow \begin{cases} (\text{Th}^{\cdot +}/\text{surface}^-) \\ (^3\text{Th}/\text{surface}) \end{cases} \quad (9)$$

5. Observation of Photoinduced Surface Species by EPR.

The suspension, following incubation of thianthrene solutions with laponite, gives a weak EPR signal due to the thermally induced radical species and corresponds to the weak absorption band at 450–600 nm in Figure 1. Photoirradiation into the CT band at 300 nm generates a strong EPR signal with a width of ~ 31.5 G (Figure 10a). The formation of the paramagnetic species on the laponite surface at room temperature is irreversible, and cessation of photoirradiation does not affect the EPR signal.

The EPR spectrum of thianthrene/laponite ($T_a = 325$ °C) irradiated at room temperature exhibits an unsymmetric structure with three lines, while EPR measurements at -196 °C show an even broader spectrum. Measurements at various levels of microwave power cannot discern whether the three lines originate from one or several paramagnetic species.

The EPR spectrum of Th$^{\cdot +}$ produced by chemical reaction in perchloric acid/acetic anhydride shows a quintet spectrum with approximate intensity ratios of 1:4:6:4:1 and a g value of 2.009 (Figure 10b). It is proposed that the protons at the 1, 4, 6, and 9 positions in thianthrene are responsible for the hyperfine structure (cf. Scheme I).[32,38] The interaction of Th$^{\cdot +}$ with its microenvironment distorts and obscures the hyperfine structure. Thianthrene radical cation perchlorate (Th$^{\cdot +}$ClO$_4^-$) solid exhibits a different EPR spectrum as shown in Figure 10c. However, if Th$^{\cdot +}$ClO$_4^-$ is loaded on dried laponite, it gives a similar EPR spectrum to that produced by photoirradiation.

(36) (a) Turro, N. J. Modern Molecular Photochemistry; Benjamin/Cummings: Menlo Park, CA, 1978; p 374. (b) Tamai, N.; Asahi, T.; Masuhara, H. Chem. Phys. Lett. **1992**, 198, 413.

(37) Nakagura, S. In Excited States, Vol. 2; Lim, E. C., Ed.; Academic Press: New York, 1975; p 322 and references therein.

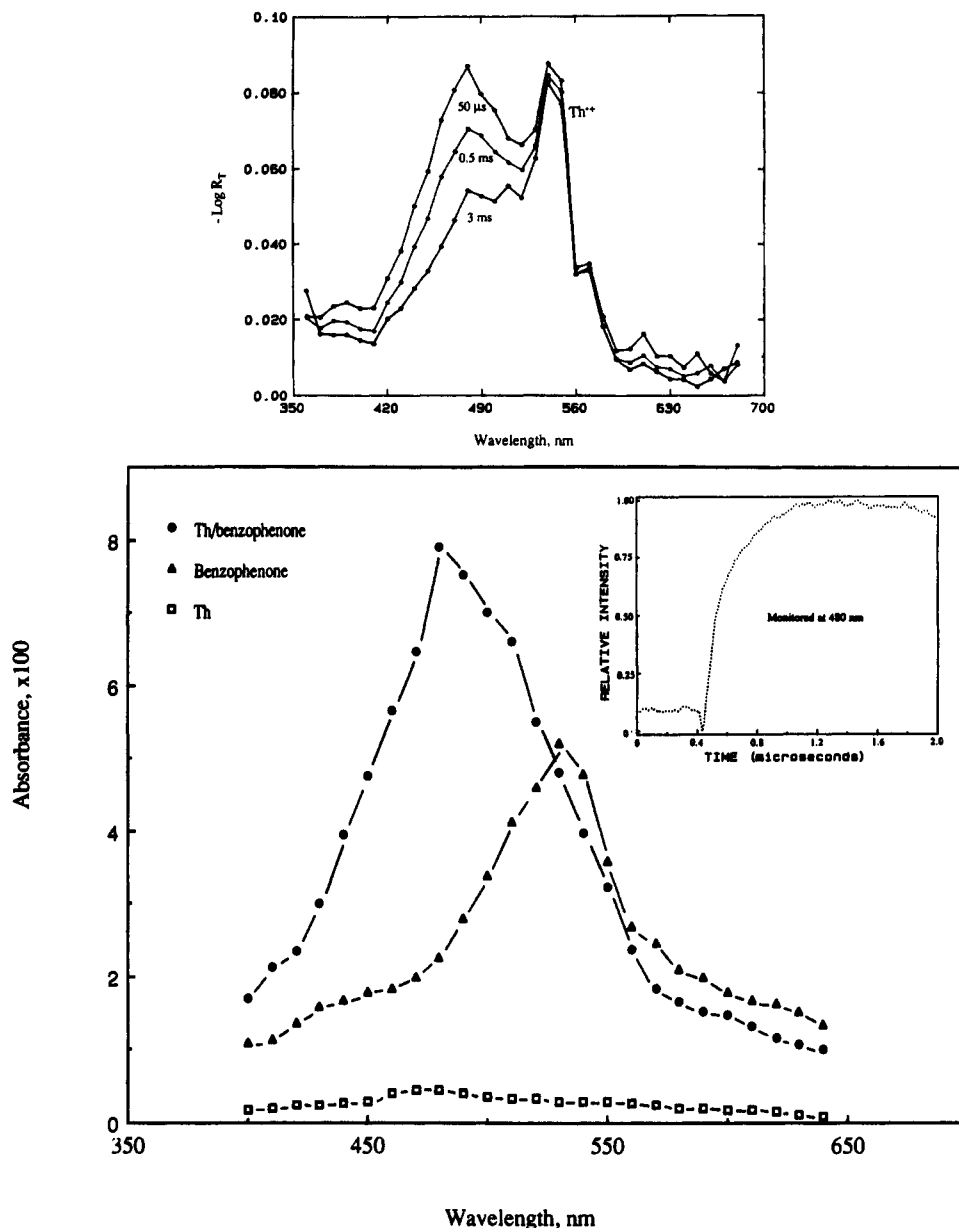(38) Shine, H. J.; Pietter, L. J. Am. Chem. Soc. **1964**, 29, 21.

Figure 9. (a) Time-resolved diffuse reflectance spectrum, at a thianthrene loading of 2.0×10^{-6} mol/g. Observed at 480 nm, the spectra were taken from top to bottom; 50 μs, 0.50 ms, and 3.0 ms after the laser flash. (b) Time-resolved transmission spectra taken 1 μs after the laser flash. N_2-purged samples, concentration: thianthrene, 1.0×10^{-4} M; benzophenone 5.0×10^{-3} M in benzene.

Figure 11 shows the effect of extended irradiation on the EPR spectra of a thianthrene/laponite sample, where the EPR signal gradually diminishes, indicating that the eventual product is diamagnetic. In the low field and the high field regions the EPR signal exhibits different behavior during extended irradiation (cf. inset in Figure 11), indicating that the EPR spectrum of Th·+ may be superimposed with a radical species derived subsequently from Th·+.

6. Hydrolysis of Photogenerated Surface Species.
Figure 12 shows a typical HPLC chromatogram of chemical products which are extracted with aqueous acetonitrile from the photoirradiated thianthrene/laponite (T_a = 325 °C). In the HPLC chromatogram fraction 1, 2, and 3 (F1, F2, F3) appear in front of the thianthrene elution. The short retention time on the reversed-phase column indicates that these products are more polar than the parent compound. The photoirradiated sample of thianthrene/laponite (T_a = 20 °C) gives an identical product spectrum

to that of an activated laponite sample but with a lower yield, indicating similar photochemical events leading to products in both cases.

By comparing the HPLC retention time with that of a reference compound, F2 is identified as thianthrene 5-oxide. The hydrolysis of Th·+ in solution producing thianthrene 5-oxide has been studied in detail[22,39-41] and obeys the half-regeneration mechanism to form the same amount of thianthrene 5-oxide and thianthrene[42,43] and a similar reaction mechanism is expected on the surface.

(39) Parker, V. D.; Eberson, L. *J. Am. Chem. Soc.* **1970**, *92*, 7488.
(40) Svanholm, U.; Parker, V. D. *J. Am. Chem. Soc.* **1976**, *98*, 997.
(41) Evans, J. F.; Blount, H. N. *J. Org. Chem.* **1977**, *42*, 976.
(42) Bard, A. J.; Ledwith, A.; Shine, H. J. Formation, Properties and Reactions of Cation Radicals in Solution in *Advances in Physical Organic Chemistry*, Vol. 13; Gold, V., Bethell, D., Eds.; Academic Press: London, 1976; p 156.
(43) Hammrich, O.; Parker, V. D. Kinetics and Mechanism of Reactions of Organic Cation Radicals in Solution in *Advances in Physical Organic Chemistry*, Vol. 20; Gold, V., Bethell, D., Eds.; Academic Press: London, 1984; p 55.
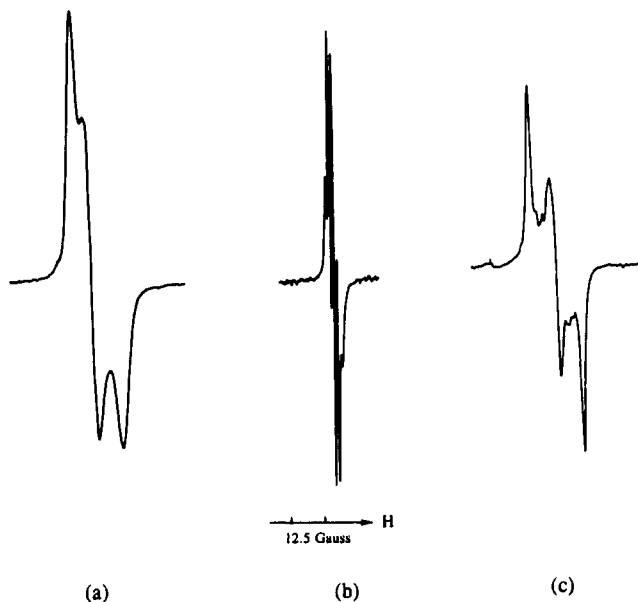
(a)   (b)   (c)

Figure 10. First derivative EPR absorption spectra recorded at room temperature. (a) Photoinduced paramagnetic species on the laponite surface; the thianthrene loading was 1.0×10^{-6} mol/g, irradiated with 3500-Å RPR lamps in the photoreactor. (b) EPR spectrum of Th$^{\cdot+}$ in perchloric acid (1 vol %)/acetic anhydride solution. (c) EPR spectrum of solid Th$^{\cdot+}$ClO$_4$. The EPR spectrum was recorded under the following conditions: microwave power, 2.0 mW; microwave frequency, $\sim$9.5 GHz; modulation frequency, 100 kHz; modulation amplitude, 1.0 G.
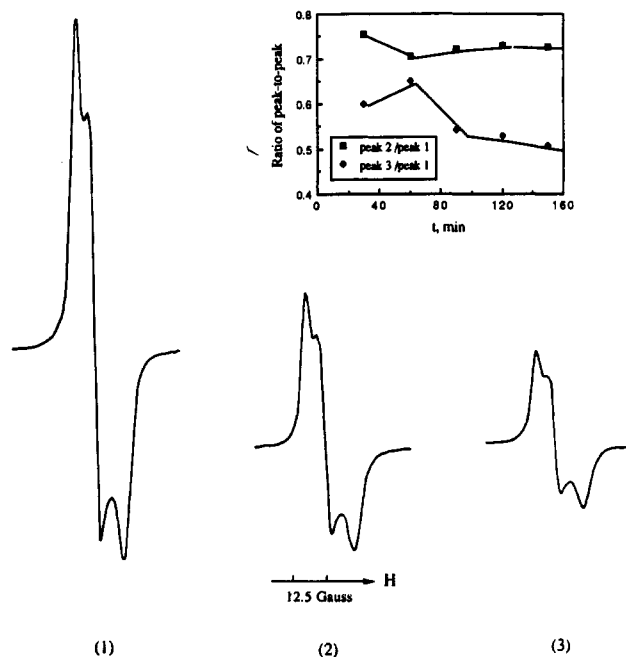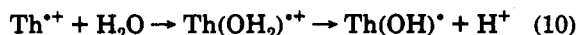

(1)   (2)   (3)

Figure 11. Effect of extended irradiation on the EPR spectra; degassed sample with loading concentration of 1.0×10^{-6} mol/g. Irradiation time: (1) 30 min; (2) 90 min; (3) 150 min. Inset: the ratio of peak to peak in EPR signals.

The Th$^{\cdot+}$ is reversibly complexed by water to form the Th(OH$_2$)$^{\cdot+}$ adduct, which may deprotonate leading to the Th(OH)$^{\cdot}$ radical.

$$Th^{\cdot+} + H_2O \rightarrow Th(OH_2)^{\cdot+} \rightarrow Th(OH)^{\cdot} + H^+ \quad (10)$$

Electron transfer from Th(OH)$^{\cdot}$ to Th$^{\cdot+}$/Th(OH$_2$)$^{\cdot+}$ produces the protonated oxide which deprotonates in water.
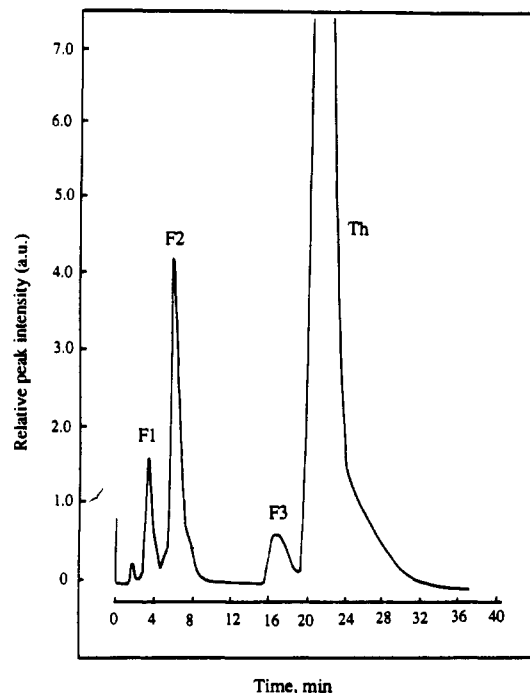

Time, min

Figure 12. HPLC chromatogram of the photoinduced chemical products. Thianthrene was adsorbed on laponite (T_a = 325 °C) in a cyclohexane solution. The reactant suspensions were irradiated in the photoreactor with 3500-Å RPR lamps. The reactant mixture was then extracted with aqueous acetonitrile (90 vol % acetonitrile), see text. The HPLC conditions were a Nova Pak C$_{18}$ column and UV absorption detector, isocratic elution with 60 vol % acetonitrile/H$_2$O, and a flow rate of 0.5 mL/min.
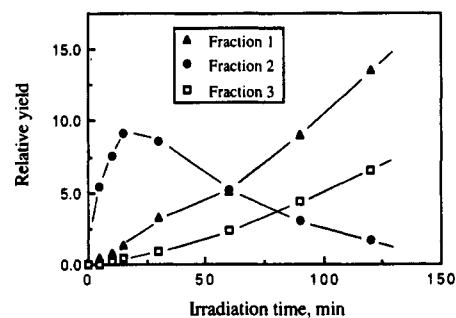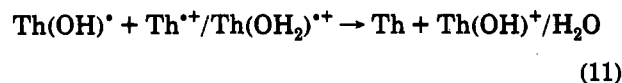

Irradiation time, min

Figure 13. Effect of extended irradiation on the relative yields of chromatographic fractions 1, 2, and 3 (see text).

$$Th(OH)^{\cdot} + Th^{\cdot+}/Th(OH_2)^{\cdot+} \rightarrow Th + Th(OH)^+/H_2O$$

$$(11)$$

$$Th(OH)^+ + H_2O \rightarrow ThO + H_3O^+ \quad (12)$$

However, on the surface other products are observed as shown in the HPLC chromatogram. The extended irradiation changes the relative yields of the products. As shown in Figure 13, the yields of F1 and F3 increase with irradiation time, while the yield of thianthrene 5-oxide decreases. After long irradiation times thianthrene exhibits only a weak peak in the HPLC chromatogram, indicating that most thianthrene is converted into products.

Conclusion

This study presents spectroscopic observations of the interaction between thianthrene and activated surface sites

on a model clay system. Physical interaction of thianthrene with surfaces generates a perturbation in the absorption spectrum, while chemical interaction leads to formation of surface complexes (CT states) and ionic species. Photoirradiation into the CT band initiates electron transfer, and radical cations are formed on the surface which are observed by diffuse reflectance and EPR spectrometry. Photoinduced electron transfer which originates from the back electron transfer of the ion pair is supported by thermal chemiluminescence studies. The extended irradiation leads to further reaction. After extraction with aqueous solutions, the surface species are converted into products, one of which is identified by HPLC as thianthrene 5-oxide. The present result shows that thianthrene adsorbed on laponite surfaces can be photochemically transformed through surface complexes into oxide.